

Article

Spatiotemporal Heterogeneity Monitoring of Cropland Evolution and Its Impact on Grain Production Changes in the Southern Sanjiang Plain of Northeast China

Tao Pan ^{1,2,3,*}  and Ru Zhang ⁴

¹ School of Geography and Tourism, Qufu Normal University, Rizhao 276826, China

² Key Laboratory of Land Surface Pattern and Simulation, Institute of Geographic Sciences and Natural Resources Research, Chinese Academy of Sciences, Beijing 100101, China

³ Center for Land Studies, Qufu Normal University, Rizhao 276826, China

⁴ School of Public Administration and Law, Northeast Agricultural University, Harbin 150030, China; s211201017@neau.edu.cn

* Correspondence: pantao@qfnu.edu.cn; Tel.: +86-18346046488

Abstract: High-speed cropland changes are taking place in Northeast China, bringing about the sustainable changes in ecological landscape and food production; however, the lack of continuous research limits the revelation of new findings in this region. The integrated approach of land migration tracking, ecological landscape and mathematical statistics was established to conduct a comprehensive survey of land change–landscape–food security in a typical grain-planting region of Northeast China to reveal new changes from 1990 to 2020. Results display that the cropland area continued to increase from 25,885.16 km² in 1990 to 31,144.46 km² in 2020, leading to the loss of forest land, grassland, water body and unused land. For cropland structure, the proportion of paddy fields in cropland increased rapidly from 7.18 to 39.53% during 1990–2020; in contrast, upland crops decreased sharply. The richness of landscape presented gradually complex characteristics with SHDI from 0.258 to 0.671 and other ecological indicators underwent similar changes with strong regularity. Total grain production displayed a continuous increase, with values from 523.79 × 10⁴ t to 1839.12 × 10⁴ t, increasing by 2.51 times from 1990 to 2020. We also revealed the contribution rate of unchanged upland crops to grain increments was the largest (i.e., 46.29%), and the conversion of internal cropland structure (i.e., the paddy fields converted from upland crops) contributed 12.17% from 1990 to 2020, showing a positive signal for food security. These new findings provide studies on land use change, ecological landscape and food security in China and abroad.

Keywords: land evolution; landscape; food security; southern Sanjiang Plain of China



Citation: Pan, T.; Zhang, R. Spatiotemporal Heterogeneity Monitoring of Cropland Evolution and Its Impact on Grain Production Changes in the Southern Sanjiang Plain of Northeast China. *Land* **2022**, *11*, 1159. <https://doi.org/10.3390/land11081159>

Academic Editor: Francisco Manzano Agugliaro

Received: 1 July 2022

Accepted: 22 July 2022

Published: 26 July 2022

Publisher's Note: MDPI stays neutral with regard to jurisdictional claims in published maps and institutional affiliations.



Copyright: © 2022 by the authors. Licensee MDPI, Basel, Switzerland. This article is an open access article distributed under the terms and conditions of the Creative Commons Attribution (CC BY) license (<https://creativecommons.org/licenses/by/4.0/>).

1. Introduction

Cropland is a bowl for feeding people on a global scale, providing essential grain and various agricultural products [1,2]. Currently, although most parts of the world have experienced different degrees of cropland expansion, the maintenance and protection of cropland area still faced many challenges [3,4] due to the interferences of the urban and industrial land expansion [5], the degradation of fertile soil [6], the excessive use of chemical fertilizers and pesticides [7], the unreasonable farming management methods [8], the abandonment of cropland [9], war conflicts [10], natural disasters [11] and extreme climate [12]. In addition to the impact of natural environment and human activities on cropland, cropland also presents the feedback to both factors, such as the soybeans that perform biological nitrogen fixation and corn affects carbon dioxide fluxes [13], paddy fields produce large amounts of methane and account for one tenth of global greenhouse gas emissions (GHGs) worldwide [14,15], and land-use change and forestry (LULCCF) also brings about an effect on climate change from the special report of the intergovernmental panel [16,17]. In the

process of interaction between cropland and environment, spatiotemporal heterogeneity monitoring of cropland evolution research continues to become a global hot issue.

For the spatiotemporal heterogeneity of cropland changes at the global scale, different continents had obvious differences. For example, the cropland area in Asia, Europe and Africa decreased; in contrast, it increased in the continents of North America, South America and Oceania from 1982 to 2011 [18]. Global distribution of cropland also displayed obvious regional characteristics at the national scale, with the top 10 countries with the largest cropland area being China, the United States, India, Russia, Brazil, Argentina, Australia, Canada, Kazakhstan and Ukraine [19]. For different cropland conversion worldwide, the increase in cropland was mainly due to the conversion of grassland and forest land, such as the regions of Central Africa, southeastern South America and East Asia [19,20]. China was a country with a large population and insufficient cropland resources [21]; thus, the food security became a national strategy [22]. China has launched a series of projects and policies to increase the cropland planting area and increase the total grain production [23,24]. For example, the food first policy in the first five-year plan and the agricultural modernization project during the reform and opening-up period have solved the problem of total food demand for the Chinese people at the end of the 20th century [25]. In the 21st century, China's cropland policies changed from quantitative expansion to rational optimization of planting types, such as high-standard farmland construction, agricultural structure measurement and supply reform, and strives to improve the types of grain planting to adapt to the changes of domestic and foreign agricultural environments while ensuring the area of cropland [25,26]. In particular, the red line for the protection of 1.8 billion mu of cropland area cannot be broken all the time [27,28]. With the continuous economic development and the continuous need for cropland, China's cropland resources were under pressure and presented complex temporal and spatial features.

In the process of the complex changes in China's cropland in time and space, Northeast China has become a grain supply base [29]. On the one hand, the natural endowments of Northeast China were relatively good, which was suitable for cropland cultivation [30,31]. The black soil with high organic content, flat terrain, rich surface and groundwater resources, humid climate and other factors were very conducive to large-scale cultivation and centralized management of cropland. On the other hand, Northeast China faced relatively low pressure of urbanization and industrialization, compared with the southeast coastal region of China. This means that the cropland in Northeast China was less used for construction land expansion, which was conducive to the protection of high-yield and high-quality cropland resources. In the past 70 years, Northeast China has been transformed from wasteland to granary through large-scale cropland expansion [32]. Therefore, Northeast China has become an important grain production base. In Northeast China, there was a leading area for farmland reform, named Sanjiang plain. In the past century, the focused region of cropland has moved from Songnen Plain to Sanjiang Plain in Northeast China [33]. In the past half century, the cover of cropland area in Sanjiang Plain has increased significantly. Since the 21st century, a large-scale reform of cropland planting structure has taken place in Sanjiang Plain. This region was a leading area for the reform of cropland structure and agricultural policies in Northeast China, acting as an indispensable role in China's grain supply market [23,34]. Considering that crop production was always affected by many natural environments, such as temperature, precipitation and soil environments, and human interferences, such as farming system, fertilization amount and management manner, we focused on the land itself to investigate crop production due to the condition that land was the basic carrier of crop production and was also the comprehensive influence results of various natural environments and human activities on crop production. However, the spatiotemporal feature of cropland evolution and its impact on ecological landscape and food production are still insufficient in the grain production base of China, which limits the revelation of current new land phenomena, as well as the relevant findings. Therefore, the objective of this study is to conduct a survey of land change–landscape–food security to reveal these new changes.

For exploring the objectives of new changes in land evolution, landscape and food safety, we defined the purpose of this study from these three perspectives in the region of the south of Sanjiang Plain, a typical farming region in Northeast China and a commodity grain base region in China. (1) From the perspective of land evolution, we investigated the temporal and spatial pattern, quantitative dynamics and change trend of land use, and tracked the cropland structure change (i.e., upland crops and paddy fields) and land conversion between cropland structure and non-cropland, with 10-year intervals from 1990 to 2020; (2) from the perspective of ecological landscape, we provided the latest landscape spatial configuration information in the process of rapid land use change, from the comprehensive landscape change, fragmentation, connectivity, dominance and edge complexity from 1990 to 2020; and (3) from the perspective of food safety, we assessed the contribution rate of the land use change process to grain production. To achieve each purpose from 1 to 3 mentioned above, we used the methodology of land migration tracking, ecological landscape and mathematical statistics, respectively. Then, in the discussion section, a comparative analysis of the new phenomenon of land change in 2020 and its previous period in China was discussed according to the new land use pattern found in this study. Moreover, a positive food security signal in the change in cropland structure in this study area was discussed. We look forward to the comprehensive analysis of land use–landscape–food security, and the findings from this study can provide practical help and a reference for relevant research.

2. Methods

2.1. Study Area

The study area focused on the southern region of Sanjiang Plain, Northeast China. The surrounding borders of this region started from the southeast end of Xiaoxing'an Mountains in the west and extended to Wusuli River in the east, and started at the Bank of Heilongjiang in the north and ended at Xingkai Lake in the south, with a total cover area of $5.53 \times 10^4 \text{ km}^2$. From the perspective of administrative division, this region consisted of 13 administrative county/city-level units (Figure 1b), along with the official names of Huachuan, Tangyuan, Baoqing, Youyi, Jixian, Jiamusi, Shuangyashan, Huanan, Yilan, Boli, Qitaihe, Hulin and Mishan, respectively.

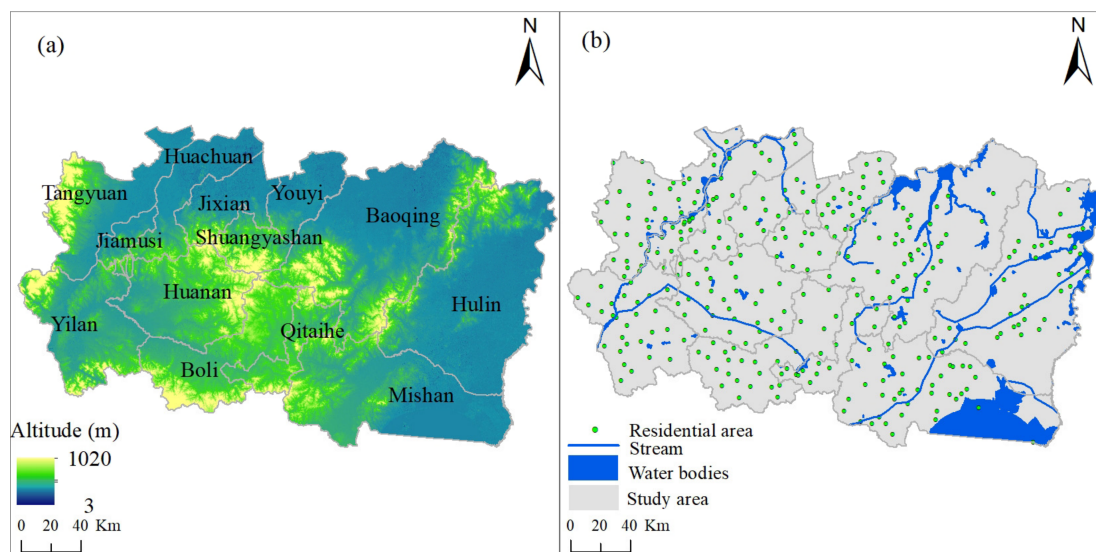


Figure 1. Spatial location map of the study area. (a) Base geographic information of the study area and (b) administrative division and elevation information.

This region belonged to a temperate humid and semi-humid continental monsoon climate. The annual sunshine duration was 2400–2500 h and the average temperature is

−21~−18 °C in January and 21~22 °C in July. The annual precipitation was 500~650 mm. In total, 75~85% of the precipitation was concentrated in the period from June to October (i.e., the crop growing season in Northeast China) to feed the crops of corn, soybean, rice, etc. In the past few decades, these cropping patterns experienced complex changes in this region that will be revealed in this study. Meanwhile, the parameters of soil types mainly contained the Argiaquoll, Calcaquoll and Aquent. These soil types included the high-quality indicator of soil organic matter, which was very suitable for the development of agriculture activities in the study area. This region was featured by the broad and flat landform (Figure 1a) and contained the dense rivers, with abundant surface flow and good water resources (Figure 1b).

2.2. Data Collection and Preprocessing

Descriptions of the main data collected in this study are summarized in the Table 1.

Table 1. Descriptions of the main data used in this study, including the indicators of characteristics, name and source.

Characteristics	Name	Source	Purpose
Basic geographic data	Land use/cover data	http://www.igsnr.ac.cn/ (accessed on 21 June 2022).	Monitoring land use changes
	Distribution map of water bodies	https://www.resdc.cn (accessed on 21 June 2022).	Assisting paddy analysis
	Distribution map of residential area	https://www.resdc.cn (accessed on 21 June 2022).	Mapping of the study area
	Administrative division	https://www.resdc.cn (accessed on 21 June 2022).	Analysis of land differences
Remotely sensed data	Digital elevation model	http://www.gscloud.cn/ (accessed on 21 June 2022).	Mapping of the study area
	Landsat Thematic Mapper	https://glovis.usgs.gov (accessed on 21 June 2022).	Land use interpretation
	Landsat Enhanced Thematic Mapper	https://glovis.usgs.gov (accessed on 21 June 2022).	Land use interpretation
	Landsat Operational Land Imager	https://glovis.usgs.gov (accessed on 21 June 2022).	Land use interpretation
	Google Images	http://www.91weitu.com (accessed on 21 June 2022).	Accuracy verification
	Faofen series satellites	http://www.gscloud.cn/ (accessed on 21 June 2022).	Accuracy verification
Grain statistics data	Crop type, yield per unit area, total production	http://tj.hlj.gov.cn/tjsj/tjnj/ (accessed on 21 June 2022).	Grain analysis

The vectorial land use data used in this study were from Institute of Geographical Sciences and resources, Chinese Academy of Sciences, with 10-year intervals from 1990 to 2010 (i.e., 1990, 2000, and 2010). The land classification system of these data consisted of 6 primary/first-level types and 25 secondary/second-level types, which provided advantages of multiple land types for land use monitoring, especially for the survey of the internal structure of cropland. Accuracy evaluation of these data on a national scale has been published; however, when it was applied to regional-scale research, data quality inspection was still an indispensable link to ensure the effectiveness and accuracy of land use status and its dynamic evaluation. In this study, man-machine digital interpretation was adopted through the combination of land data and remote-sensing images to check data quality.

For the remote-sensing images, United States Geological Survey (abbreviation: USGS, official website: <https://www.usgs.gov/> (accessed on 21 June 2022)) provided all Landsat images [35]. According to the crop phenological calendar in the study area, the images of crop growth season (i.e., from May to September of each year) were downloaded,

considering that it was easy to distinguish land types of vegetations, buildings and bare soils in remote-sensing images during this period. An image synthesis approach was used by false color composite due to this method being conducive to the land use type interpretation of the professional geographical knowledge. Moreover, we downloaded high-resolution google satellite images to further view the land types of the images. After that, we superimposed land use data and corresponding images together to check the quality and correct the wrong land covers of each land use type by professional knowledge distinguishing from color, texture and shape in the images. Then, the stratified random sampling approach was applied for accuracy evaluation, with the accuracy of 96.28, 96.63 and 95.15% in 1990, 2000 and 2010, respectively. After that, based on the 2010 land data, we superimposed these onto the 2020 Landsat images using manual visual interpretation. The combination of the high-resolution images and stratified random sampling approach was used for accuracy evaluation, with a value of 97.73% in 2020. A schematic diagram of land use/cover data inspection in 1990, 2000 and 2010 and production in 2020 is provided below (Figure 2).

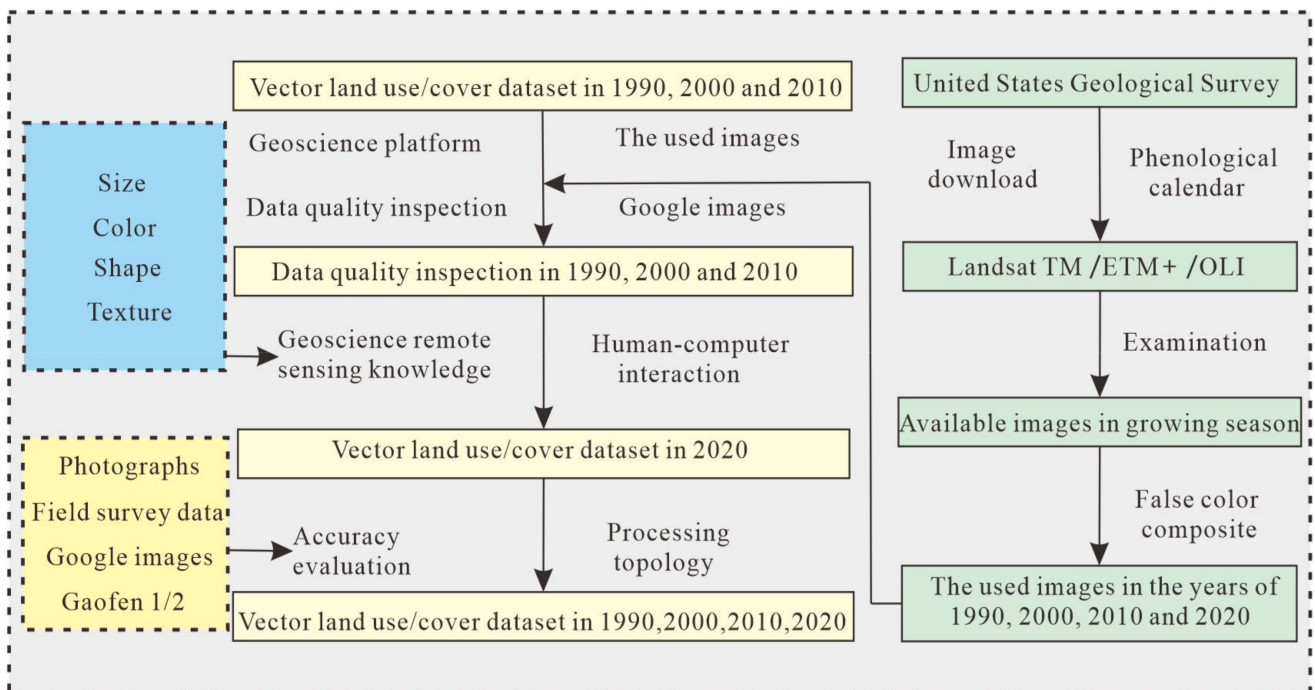


Figure 2. Schematic diagram of land use/cover data inspection in 1990, 2000 and 2010 and production in 2020.

The basic geographic information data mainly contained the administrative division of the study area that was used for the statistical analysis of land use change and grain yield, and the digital elevation model and river distribution that was used for the geographic location mapping of the study area. In addition, the annual grain census data were mainly from the statistical yearbooks, and we also obtained the corresponding archived data of food crops from local government departments and universities, considering that the time span of this study was 30 years (i.e., 1990–2020) and the previous statistical yearbook data were insufficient.

2.3. Spatial Monitoring Method of Land Change

A land migration tracking approach was applied to carry out land use change analysis. Compared with conventional land monitoring methods, such as land use dynamic degree, the land migration tracking approach can not only be used to analyze the temporal characteristics, trends and ranges of land use, but also provide the source and loss of each

land use type. This means that we can explore the area increment of each land use type and the contribution rate of other land types to this increment to investigate the source of area increment for each land utilization type, as well as the same for the loss of each land use type. The principle of this method is displayed below [36]:

$$S_{ij} = \begin{pmatrix} S_{11} & S_{12} & \cdots & S_{1n} \\ S_{21} & S_{22} & \cdots & S_{2n} \\ \vdots & \vdots & \vdots & \vdots \\ S_{n1} & S_{n2} & \cdots & S_{nn} \end{pmatrix}$$

where S_{ij} was the land use region that converted from the land use type i at the beginning of the study to the land use type j at the end of the study period, and n was the number of land use types in the specific regions.

In this study, we processed the land migration investigation statistics on a professional land information processing platform. Land use vector data of the two phases were overlapped by professional tool commands on this platform so that the attribute tables of the two periods of data could be combined into one table. Then, the PivotTable function was used to split the land attribute tables and area value to obtain the type and area matrix of two phases of land changes. In this matrix, the indicators of transfer in, transfer out, net change of each land use type and its interaction with other land use types were clearly presented. We counted the changes in these indicators to carry out the land migration tracking.

2.4. Selection and Analysis of Ecological Landscape Index

Landscape ecological indicators can often express the spatial allocation changes in land use, so they were often used in land-related research and acted as an essential role in the landscape ecology field. We used landscape ecological indicators to investigate the changes in landscape in the study area and the concerned land types. From this point of view, we searched the indicators of landscape level and type level according to the user guide of landscape indicators. This user guide can provide the equation, English expression, abbreviation and ecological meaning characteristics of each landscape indicator, which has been widely used as the indispensable reference source for ecological landscape research [37]. In the user guide, the same landscape indicator had multiple meanings, and the same meaning can be expressed by multiple indicators. In combination with the land use change in the study area and the ecological meaning of landscape indicators, Shannon's diversity index was firstly selected. The purpose of selecting this indicator was to analyze whether the whole landscape change in the study area was complicated or simplified. Then, to explore the spatial advantages of a certain land use type over other land types in the process of land use change, the largest patch index was used, showing the spatial distribution and dominance of a certain land use type [38], as well as the connectance index for the connectivity [39]. With the changes in different land use types, the ecological landscape was often broken, and patch density expressed this meaning succinctly and directly; it was applied to this survey. Finally, to determine how the edge shapes of land use types change under the background of drastic land use change, landscape shape index was used to investigate the issue. From the landscape perspective of comprehensive change, fragmentation, connectivity, dominance and edge complexity, we have selected and calculated the above five landscape ecological indicators. The full names, abbreviations and equations of each indicator are listed in the following table (i.e., Table 2) according to the user guide of landscape indicators [40].

Table 2. Full names, abbreviations and equations of each landscape ecological indicator.

Full Names	Abbreviations	Equations
Patch Density	PD	$PD = \frac{n_i}{A}(10,000)(100)$

Table 2. Cont.

Full Names	Abbreviations	Equations
Largest Patch Index	LPI	$LPI = \frac{\max_{j=1}^n(a_{ij})}{A} (100)$
Landscape Shape Index	LSI	$LSI = \frac{0.25 \sum_{k=1}^m e_{ik}^*}{\sqrt{A}} \text{ or } = \frac{0.25E^*}{\sqrt{A}}$
Connectance Index	CON	$connect = \left[\frac{\sum_{j \neq k}^n C_{ijk}}{\frac{n_i(n_i-1)}{2}} \right] (100)$
Shannon's Diversity Index	SHDI	$SHDI = - \sum_{i=1}^m P_i \ln(P_i)$

2.5. Contribution Rate of the Different Land Use Transformations on Total Grain Production

In this section, we only analyzed the impact of different land use type changes, such as the land transformations among paddy fields, upland crops and noncropland, on the contribution rate of the total production. The annual grain census data were mainly from the statistical yearbooks, including the crop planting types and yield per unit area. In the meantime, we collected the archived data on food crops and yields from local governments and state farms to further improve the food data over a 30-year span for the accurate statistics and analysis. After collecting these grain data, the next process was to convert different crop yields to the internal cropland structure yield (i.e., paddy fields and upland crops) using the weighting method. For the paddy fields, we can directly obtain the yield per unit area of paddy fields from the statistical yearbook to guide the relevant analysis. For the upland crops, we gave the weight coefficient corresponding to the area according to the area of different crops to the total area of upland crops, and the sum of weight coefficients was 1. Then, the weight coefficient of each upland crop was multiplied by its corresponding yield per unit area to obtain the yield per unit area of all the upland crops. Grain yield was often affected by many factors, especially the natural environment, such as drought, high temperature, hail, flood, low temperature, etc. When the rain was abundant and the temperature was appropriate, crop yield was generally good (i.e., the bumper harvest year). On the contrary, when the natural disasters, such as drought, flood, hail and low temperature, occurred, the unit yield of grain reduced. Other years were usually normal years. Among the bumper harvest year, disaster year and normal year, the crop yield/production presented the difference. Considering that the period of the obtained and created land use data in this study was 10-year intervals from 1990 to 2020, the corresponding time of the grain yield/production used in this study was calculated with the recent 5-year average value to eliminate the interference of uncertain factors on grain yield/total production. According to our survey and local archives, the 5-year average value for the specific years (i.e., 1990, 2000, 2010 and 2020) can effectively reflect the real unit yield and total production of grain. Then, the grain yield/production in 1990, 2000, 2010 and 2020 was obtained, which was used for statistical analysis and calculation in the study. Furthermore, for the calculation of annual grain production increment, the 5-year average production for the years of 1990, 2000, 2010 and 2020 mentioned above was used. We obtained the grain production changes of each period (i.e., 1990–2000, 2000–2010 and 2010–2020) by subtracting the first year (i.e., the 5-year average) from the last year (i.e., the 5-year average), and the grain production change in each period was further averaged to each year of each period to obtain the annual average grain change in 1990–2000, 2000–2010 and 2010–2020, respectively.

Through Geographic Information System software platform, we used the spatial re-classification, extraction and clipping functions to merge different land use types to achieve the purpose of obtaining the compressed land use types, which was guided to classify land use transformation effect on grain production in this study [41]. As forest land,

grassland, water, construction land and unused land were not planted with grain, we called it noncropland. In the land classification system used in this study, cropland was further divided into paddy fields and upland crops, and these two sub-categories of cropland were adopted. Taken together, the land use types were classified to three categories, namely, noncropland, paddy fields and upland crops. By combining mathematical statistics and land migration tracking approach, we obtained the following types of land change to explore the impact of land change on food production, including the unchanged upland crops, upland crops transferred into noncropland, upland crops transferred into paddy fields, unchanged paddy fields, paddy fields transferred into noncropland, paddy fields transferred into upland crops, unchanged noncropland, noncropland transferred into upland crops and noncropland transferred into paddy fields. Then, the impact of each land change on grain production was calculated and analyzed over the studied period.

3. Results

3.1. Analysis of Land Use in the Quantitative and Spatial Changes in the Southern Sanjiang Plain of Northeast China from 1990 to 2020

During the period from 1990 to 2020, the land use change trend in the study area showed two completely opposite directions according to our statistics of the vector data, accompanied by the increased land types of cropland and construction land, and the decreased land types of unused land, water, grassland and forest land. For the increments, the coverage of cropland area continuously increased from 25,885.16 to 29,611.58 km², 30,391.87 km² and 31,144.46 km² (Table 3) in the studied years of 1990, 2000, 2010 and 2020, with the changed areas of 3726.42, 780.29 and 752.58 km² in the period of 1990–2000, 2000–2010 and 2010–2020, respectively. Correspondingly, the land reclamation rate (i.e., the proportion of cropland in the corresponding area of the whole administrative region) constantly increased from 46.80 to 53.54, 54.95 and 56.31%, with the total increment of 9.51%, showing that the proportion of cropland in the study area has exceeded half of the total area. Another land use type that continued to increase was construction land under the backgrounds of urbanization and industrialization from 1990 to 2020, with the total areas of 1274.97 km² in 1990 to the 1411.19 km² in 2020, indicating the total increment of 136.22 km². In contrast, trend of cropland and construction land, the grassland, water and unused land displayed the characteristics of continuous loss in the studied period. Among them, the largest loss area occurred in unused land, followed by grassland and water, with the net change area of −1966.33 km², −1897.48 km² and −189.10 km², respectively. As for the forest land, although its total area also showed a downward trend, its change area displayed a unique feature by fluctuation reduction, with the changed areas of −1314.38 km², +15.70 km² and −43.93 km² in the period of 1990–2000, 2000–2010 and 2010–2020, respectively. Therefore, the land use change pattern in the whole study area was dominated by the expansion of cropland, with the changed area of +5259.29 km² from 1990–2020.

Table 3. The first-class land use area in 1990, 2000, 2020 and their dynamic changes with 10-year intervals from 1990 to 2020 in the southern region of Sanjiang Plain (unit: km²).

	1990	2000	2010	2020	1990–2000	2000–2010	2010–2020
Cropland	25,885.16	29,611.58	30,391.87	31,144.46	3726.42	780.29	752.58
Forest land	17,025.98	15,711.60	15,727.31	15,683.38	−1314.38	15.70	−43.93
Grassland	4000.38	2646.55	2335.84	2102.90	−1353.82	−310.71	−232.94
Water	2789.25	2713.83	2668.86	2600.15	−75.42	−44.97	−68.71
Construction land	1274.97	1312.93	1343.76	1411.19	37.96	30.83	67.43
Unused land	4332.06	3311.31	2840.17	2365.74	−1020.75	−471.14	−474.43
Total Area	55,307.80	55,307.80	55,307.80	55,307.80	0.00	0.00	0.00

For the spatially evolutionary pattern of land use (Figure 3), cropland presented a divergent, disorderly and rapid expansion to all directions. Construction land was mainly

based on the original center and expanded towards the adjacent surrounding areas. The loss of forest land mainly occurred in the middle and northeast of the study area. Moreover, a large amount of sustained grassland loss was monitored in the eastern part of the study area. Meanwhile, the unused land displayed divergent disappearance. In general, the land use pattern in the study area featured the complex change characteristics.

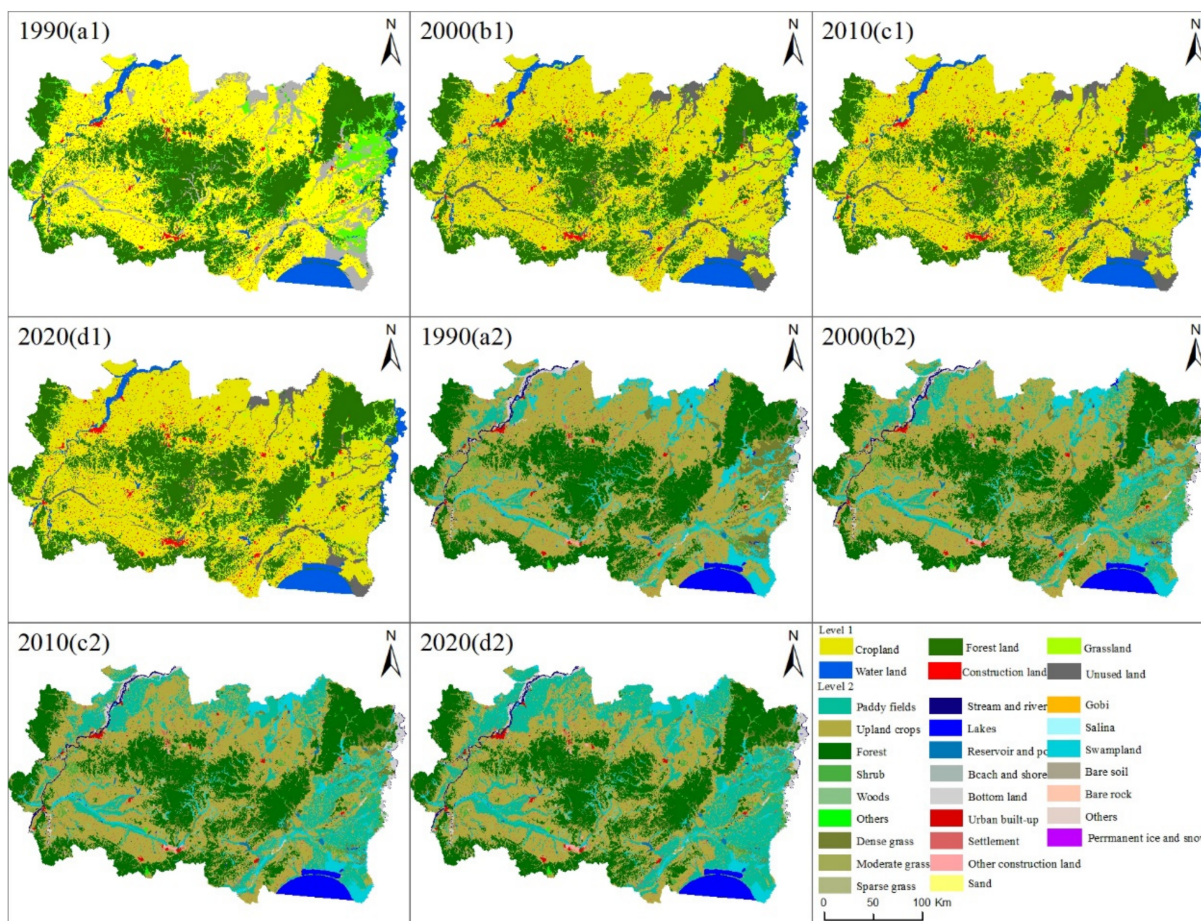


Figure 3. Spatial evolution map of land use in the study area in the years of 1990, 2000, 2010 and 2020, respectively. Note: Level 1 of land types was (a1–d1) and the corresponding level 2 was (a2–d2).

3.2. Analysis of Continuous Cropland Structure Change and Land Conversion from 1990 to 2020

3.2.1. Analysis of Spatiotemporal Characteristics in Cropland Structure from 1990 to 2020

Although cropland in the study area continued to increase from 1990 to 2020, its structure, including the paddy fields and upland crops, displayed the different evolutionary characteristics. Specifically, the coverage area of paddy fields in 1990 was 1857.54 km²; then, a sustained, rapid, and intense paddy field expansion was monitored (Figure 4), with areas of 5513.41, 8835.85 and 12,311.63 km² in 2000, 2010 and 2020, respectively, which indicated the paddy field area in the last year was 6.63 times bigger than that in the initial year of the study. In contrast, the total coverage area of upland crops decreased from 1990–2020, with a fluctuating feature, namely, the area of upland crops slightly increased by 70.55 km² during 1990–2000, but a large-scale loss of the area occurred after 2000 with a change in area of −2542.16 and −2723.20 km² during the periods of 2000–2010 and 2010–2020. On the whole, the net changing areas of paddy fields and upland crops were +10,454.10 and −5194.81 km² over the studied period, showing the completely opposite trend characteristic. Moreover, this change also brought about the change in the proportion of paddy fields/upland crops to total cropland, with corresponding values of 7.18 vs. 92.82% in 1990 to 39.53 vs. 60.47% in 2020.

Under the differently changing backgrounds of cropland structure, the spatial change patterns also displayed the differences. For paddy fields, its distribution was mainly scattered in 1990. The main accumulation regions were located on the west of the study area where the rivers flowed. After 1990, taking the rivers as the main supporting area, paddy fields began to expand towards adjacent land types. Further, paddy field expansion began to show a trend of being far away from rivers under the adaptation of advanced irrigation practices, on the condition that the surrounding rivers were already paddy fields. In 2020, paddy fields had already been concentrated in the western, northern and eastern parts of the study area. For upland crops, upland crops were mainly distributed by centralized and contiguous patterns in the study area in the initial year. Then, widespread loss of upland crops happened during 1990–2020. At last, upland crops were mainly only distributed in the western, northern and southern parts of the study area.

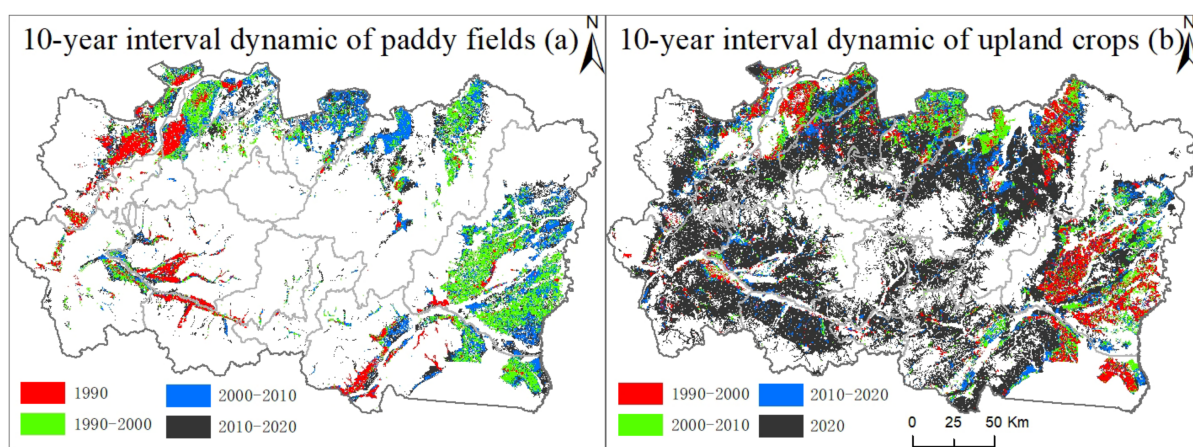


Figure 4. Spatial pattern of cropland structure from 1990 to 2020. Note: (a) and (b) were the 10-year interval dynamic of paddy fields and upland crops, respectively.

3.2.2. Analysis of Land Migration Tracking in Cropland Structure from 1990 to 2020

A land migration tracking approach can clearly show the source, loss and net change from each land use type, which was conducive to revealing the rapidly changing mechanism of paddy fields and upland crops. The statistics of land migration tracking in the study area from 1990 to 2020 is provided in the Table 4.

Table 4. Areas of land use transformation among the land types of forest land, grass land, water land, construction land, unused land, paddy fields and upland crops from 1990 to 2020 (unit: km²).

	Forest Land	Grass Land	Water Land	Construction Land	Unused Land	Paddy Fields	Upland Crops	1990 Total
Forest land	15,584.10	18.92	0.41	4.00	1.61	100.74	1316.20	17,025.98
Grassland	15.73	2060.81	0.69	4.91	2.20	1164.63	751.42	4000.38
Water land	0.30	0.27	2572.28	1.49	19.08	139.63	56.20	2789.25
Construction land	0.17	0.00	0.04	1266.34	0.00	6.69	1.72	1274.97
Unused land	1.56	3.19	3.20	3.43	2314.94	1615.09	390.65	4332.06
Paddy fields	0.04	0.48		7.80	0.52	1816.03	32.67	1857.54
Upland crops	81.47	19.24	23.53	123.22	27.38	7468.82	16,283.97	24,027.63
2020 Total	15,683.38	2102.90	2600.15	1411.19	2365.74	12,311.63	18,832.82	55,307.80

According to Table 4, the coverage of unchanged paddy fields during 1990–2020 was 1816.03 km², which accounted for 97.77% of the total paddy field area (i.e., 1857.54 km²) in the initial year (i.e., 1990), indicating that the original paddy field coverage was very stable. In this case, the loss of paddy fields was very weak, with total areas of 41.50 km². Among them, the converted area from paddy fields to upland crops was dominant, namely, 32.67 km², followed by the conversion of paddy fields into construction land, with an area of 7.80 km². So, the area of paddy field loss to other types was only 1.04 km², which can be

basically ignored. Meanwhile, the inflow area of paddy field was very large, with a net area of 10,454.10 km² from 1990 to 2020. The main contribution of paddy field increase came from the conversion of upland crops, with a total area of 7468.82 km², which accounted for 71.44% of the total increment of paddy fields. So, the increment of paddy fields mainly came from the internal conversion of cropland, and the contribution from noncultivated land was sorted by unused land, grassland, water, forest land and construction land, with the areas of 1816.03, 1164.63, 139.63, 100.74 and 6.69 km². Therefore, the original paddy fields were stable and the new paddy fields mainly came from the conversion within the cropland and from unused land and grassland among the noncroplands.

For the upland crops, the coverage of unchanged upland crops during 1990–2020 was 16,283.97 km². This value accounted for 67.77% of the total upland crop area (i.e., 24,027.63 km²) in the initial year (i.e., 1990). The loss of upland crops was mainly transferred to paddy fields, which occupied 96.45% of the total loss, followed by the conversion to construction land due to the expansion of urban, rural and industrial land. The newly increased area of upland crops was also multi-source, with a total area of 2548.85 km². Among them, the total contribution of forest land and grassland was 81.12%.

3.3. Analysis of Landscape Evolution Process at Different Scales from 1990 to 2020

At the landscape scale, under the comprehensive change in cropland structure from 1990 to 2020 (Table 5), the richness of landscape presented gradually complex characteristics with Shannon's diversity index (SHDI) from 0.258 to 0.481, 0.603 and 0.671 in the years of 1990, 2000, 2010 and 2020, respectively. The rich landscape also led to the fragmentation of patch density (PD), and its value increased 4.55 times from 0.158 in 1990 to 0.718 in 2020. This change weakened the connectivity among different land types, bringing about the continuous decrease in connectivity index from 0.206 to 0.074, 0.058 and 0.043 in each studied year. Due to the fragmentation of patches and the weakening of patches' connectivity, the dominance of all patches continues to decrease (i.e., the largest patch index (LPI) from 39.918 in 1990 to 23.261 in 2020) and the degree of edge combination of patches continues to complicate, with landscape shape index (LSI) from 82.207 to 121.457, 125.107 and 127.942 in the years of 1990, 2000, 2010 and 2020, respectively. The landscape of the whole study area has undergone complex changes with strong regularity from 1990 to 2020.

Table 5. Landscape pattern statistics of cropland structure change at landscape and type scales during the period of 1990–2020.

Scales	Land Types	Year	PD	LPI	LSI	CONNECT	SHDI
Landscape	Cropland	1990	0.158	39.918	82.207	0.206	0.258
		2000	0.542	34.901	121.457	0.074	0.481
		2010	0.673	33.167	125.107	0.058	0.603
		2020	0.718	23.261	127.942	0.043	0.671
Types	Paddy fields	1990	0.083	5.882	56.951	0.064	
		2000	0.211	12.036	123.673	0.069	
		2010	0.204	18.597	126.093	0.070	
		2020	0.189	19.697	132.398	0.171	
	Upland crops	1990	0.075	39.918	81.492	0.249	
		2000	0.331	34.901	123.643	0.076	
		2010	0.469	33.167	132.428	0.056	
2020		0.528	23.261	136.529	0.041		

At the land-type scale, the rapid paddy field expansion has formed a concentrated and contiguous paddy field spatial pattern, bringing about the continuous improvement of patch superiority, with LPI values from 5.882 in 1990 to 12.036, 18.597 and 19.697 in 2000, 2010 and 2020. In contrast, the massive loss of upland crops led to the decrease in patch dominance, accompanied by LPI values of 39.918 in 1990, and then to 34.901, 33.167 and 23.261 in 2000, 2010 and 2020. The data showed that the patch dominance

of upland crops was still stronger than that of paddy fields in 2020. Correspondingly, the connectivity of paddy fields continuously improved, but the value of upland crops continuously decreased. Meanwhile, the invasion of paddy fields into upland crops made the spatial mosaic pattern more obvious between these two types, bringing the complexity of their spatial landscape shape, with LSI values of 1.68 greater in upland crops and 2.32 in paddy fields. The landscape ecological indicators of upland crops and paddy fields presented both common change trends and difference in differentiation from 1990 to 2020.

3.4. Analysis of Total Grain Production and Its Impacts from the Evolution of Rapid Cropland Structure from 1990 to 2020

3.4.1. Crops' Total Grain Production Changes and Their Evolutionary Processes in the Study Area

For the analysis of grain production changes in different years, the Kruskal–Wallis test approach was first used in this section to test whether there was significance between the changes in years and the changes in crop productions, and the results displayed that $p > 0.05$, meaning that the changes in years and in crop productions had no significant correlation. Then, we used the 5-year average value (i.e., common trend analysis method) to conduct the grain production statistical analysis.

Total grain production in the study area displayed a continuous increase, with 5-year average production of 523.79×10^4 t, 1024.13×10^4 t, 1721.02×10^4 t and 1839.12×10^4 t in 1990, 2000, 2010 and 2020, respectively (Figure 5), showing that the total grain production increased by 2.51 times over the study period. The increases in total grain production means that more people can be supported, which showed a positive signal for food security. However, the increase in total grain production showed different stages, with the changing values of $+500.34 \times 10^4$ t, $+696.89 \times 10^4$ t and $+118.10 \times 10^4$ t in the periods of 1990–2000, 2000–2010 and 2010–2020, respectively. The data displayed that the total grain production featured a continuous increase, with the average annual growth of 50.03×10^4 t and 69.69×10^4 t in the first two stages, while the average annual growth suddenly dropped to 11.81×10^4 t in the last period, which was mainly caused by the different evolution of crops and their yield per unit area in the period of 1990–2000, 2000–2010 and 2010–2020, respectively. The detailed explanation of this phenomenon is found below.

In 1990, low-yield soybean (i.e., 1825.77 kg/ha) accounted for nearly half (i.e., 47.87%) of the cropland area and was the dominant crop (Figure 5b). In contrast, the proportion of high-yield paddy fields and corn only accounted for 7.18% and 18.11%, respectively.

Then, in the first stage (i.e., 1990–2000), the planting area of high-yield corn and paddy fields increased, with the proportion in cropland increasing to 21.61% and 18.62% in 2000. In contrast, soybean reduced to 30.77%. The large-scale expansion of high-yield corn and paddy fields and the rapid shrinkage of low-yield soybean effectively promoted the growth of total grain production in this stage.

Similarly, in the second stage (i.e., 2000–2010), the planting area of low-yield soybean continued to shrink to 26.12%. In contrast, the high-yield corn and paddy fields evidently increased, with the proportion in cropland increasing further to 35.92% and 29.07%, respectively, which rapidly increased the total grain production.

Differently, in the third stage (i.e., 2010–2020), low-yield soybean began to return to large-scale planting (i.e., from 26.12 to 38.47%) again, while the proportion of low-yield corn decreased from 35.92 to 21.12%. The planting area of high-yield paddy fields continued to increase from 29.07 to 39.53%. Comprehensive change in crops and their yields still led to the increase in total grain production.

During the whole research period, the proportion of other crops in cropland continued to decrease, with values from 26.84 to 0.88% (Figure 5b). Therefore, in the process of increasing the total grain production, the crops experienced complex structural changes in the study area from 1990 to 2020.

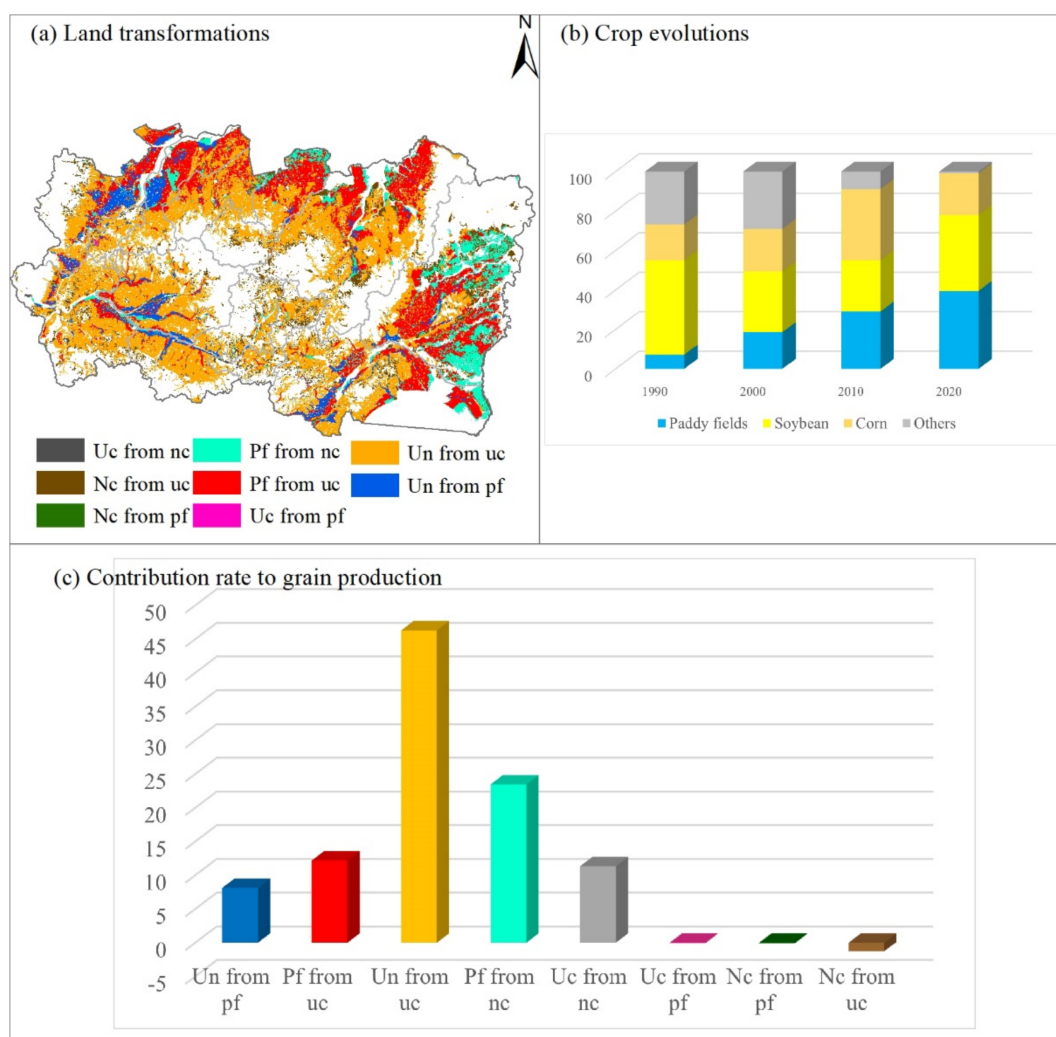


Figure 5. Landscape pattern statistics of cropland structure change at landscape and type scales during the period of 1990–2020. Abbreviation: Uc from nc: upland crops converted from noncropland, Nc from uc: noncropland converted from upland crops, Nc from pf: noncropland converted from paddy fields, Pf from nc: paddy fields converted from noncropland, Pf from uc: paddy fields converted from upland crops, Uc from pf: upland crops converted from paddy fields, Un from uc: unchanged upland crops, and Un from pf: unchanged paddy fields.

3.4.2. The Effects of Different Cropland Evolution on Total Grain Production from 1990 to 2020

For the measure of the degree of agreement between changes in grain production and the changes in cropland, we conducted a fitting analysis of the total grain production and the total cropland area, obtaining the values of $Y = 0.0351X + 247.78$ ($R^2 = 0.8617$, $p < 0.05$), indicating that the results had good fitting and passed the significance test. In the process of continuous evolution of cropland planting structure and grain yield per unit area (Figure 5a,b), the total grain production in the study area changed naturally. According to the changing crops' yield per unit area, we investigated the effects of different cropland structure evolution processes on total grain production (Figure 5c). For the paddy fields, the contribution rate of unchanging paddy fields to grain increments was 8.12% due to the increasing yield per unit area from 4475.40 kg/ha to 8566.78 kg/ha in the past 30 years (i.e., 1990–2020). Meanwhile, the transformation of noncropland into paddy fields also had a positive impact on food security, with a contribution rate of 23.46%. Moreover, the improved grain production from upland crops to paddy fields was 12.17%. For the upland crops, the contribution rate of unchanging upland crops to grain increments reached

46.29%, considering that upland crops were the main cropland type in the whole study period and the increases in upland crops' unit yield. This was also the type of cropland structure with the largest contribution rate to grain output from 1990 to 2020. In addition, the transformation from noncropland to upland crops also contributed 11.33% of the total grain increment. To sum up, these changes all showed the positive contributions to food security. Meanwhile, the transformations of paddy field into upland crops, paddy fields into noncroplands and upland crops into noncropland displayed the negative feedback effect.

4. Discussion

4.1. A Comparative Analysis of the New Finding of Land Change in 2020 in the Study Area and Its Previous Period in China

In this study, we made a comprehensive analysis of the land use change from 1990 to 2020, and the temporal and spatial evolution pattern of cropland continued to be the main land use type in the study area. An important finding was that the total coverage of cropland area still continued to increase, with the changing areas of 3726.42 km², 780.29 km² and 752.58 km² in the period of 1990–2000, 2000–2010 and 2010–2020, respectively. We called it an important discovery for two reasons. One was the continuous increase in cropland area in the study area. As we know, China's cropland has undergone drastic changes in the past three decades [34,42]. The overall evolution pattern of cropland in China was as follows: the cropland area in the southeast coastal area (i.e., Southeast China) decreased [43], and the area of cropland was further weakened by returning farmland to forest and grassland policy in the middle part (i.e., Central China) [44]. As a result, Northern China (i.e., Northwest China and Northeast China) has become an irreplaceable region for new expansion of cropland [34,45]. Especially in the Northeast China region, which was called "the northern wilderness region" in the past and called "northern granary" now [46], meaning that large-scale wasteland has been turned into cropland. Northeast China has now become an important food production base in China. Therefore, in the case of large-scale expansion of cropland in the whole northeast region (i.e., Northeast China), the phenomenon of cropland increases naturally occurred in our study area, and cropland area statistics in this study also reflected this view.

However, on the other hand, our new findings just happened in croplands at different time nodes, namely, the total cropland coverage in the study area increased by 752.58 km² 2010–2020 [47]. In contrast, in the same period, the total coverage of cropland area in Northeast China did not increase continuously, but decreased by over 200 km² across the whole region of Northeast China. Considering that China's total population accounted for about 22% of the world's population and the cropland resources only accounted for 7% of the world's cropland, food security continued to be the focus of China [48]. In 2010–2020, when the total area of cropland in the northeast granary of China decreased, the finding that the increase in total cropland coverage in the study area was particularly important for the role of the northeast as a granary and even China's food security [49,50].

4.2. A Positive Food Security Signal in the Change in Cropland Structure in Northeast China

Our survey found that the total grain production in the study area has increased by 3.51 times in the past 30 years, amounting to the 1839.12×10^4 t in the ending year, showing the positive food security signal in the change in land use. In fact, in the past three decades, China's grain production has been growing continuously [51,52]. The increases in the total grain production in our study area were a microcosm of the effectiveness of China's food security strategy [52–54]. Behind the grain growth, the reason for grain production increase, on the one hand, was the continuous increase in grain yield per unit area through a series of projects and agricultural policies [55,56], such as high-yield seed research and development, fertilizer and pesticide use, improved agricultural management, cropland structure circulation policy, land remediation projects, high-standard farmland construction projects, agricultural water conservancy projects, etc. These policies and projects have significantly increased the output of crops, thereby promoting grain production. This

phenomenon was also confirmed in our study area, specifically, the yield per unit area of paddy fields, corns and soybeans was 8566.78, 9810.13 and 2460.70 kg/ha, which were 1.91, 2.16 and 1.55 times greater than that of the initial year.

In addition to the increases in grain yield per unit area, China's cropland planting structure has experienced a series of complex temporal and spatial changes, rather than just tracking the increase in the yield of the certain grain crop [57–60]. Our research area located in the commodity grain production base and the change in crop planting structure in the study area can reflect the China's cropland planting structure trend faster than that in other agricultural planting areas. We found that, in the first stage, the proportion and scale of corn planting increased. In the second stage, corn and rice paddy continued to expand. In these two stages, the scale of soybean planting continued to shrink. In the third stage, the rice paddy was still expanding, but the planting scale of soybean began to recover and the planting of corn began to decrease. Such changes in planting structure have fully combined China's accession to the world trade organization, the reform of cultivated land side supply and international agricultural trade conflicts. In this process, China's total grain production always maintained an increasing trend.

4.3. Grain of Our Study Area Is Not Only Served Locally, but Also Exported to Other Parts of the World

Food security was always related to the total population. From 1990 to 2020, the total population of China was 1.16 billion, 1.30 billion, 1.37 billion and 1.41 billion in the years of 1990, 2000, 2010 and 2020, respectively, indicating that the population increase during the studied period was 0.25 billion, along with the total population growth rate of 21.72% from 1990 to 2020 in the whole region of China. The continuous increase in population will inevitably require more food supply. The Chinese government has implemented many cropland protection projects and policies, such as the balance of cropland occupation and compensation, in which, for each piece of cropland occupied, it was necessary to compensate the same area of cropland in other areas to ensure sufficient arable land area for food production. In the context of the increasing demand for food from the increasing population [61], China's grain production bases played an indispensable role in ensuring food security. Our study area was one of China's grain production bases and we found that the total grain production in the study area continued to increase from 1990 to 2020, with a value of 523.79×10^4 t in the initial year and 1839.12×10^4 t in the last year, showing that the total grain production increased by 251.12%. The data displayed that the growth rate of grain in the study area was much higher (251.12 vs. 21.72%) than that of China's population. According to our survey, the grain in our study area, named "Northeast rice in China", can not only meet the needs of local residents in Northeast China, but also was delivered to all regions of China, such as the cities of Beijing (i.e., North China), Shanghai (i.e., East China) and Guangzhou (i.e., South China). In addition to being widely sold in China, "Northeast rice" was also transported abroad. Abroad, most of the rice entered the supermarkets of Chinese merchants, and the rice was very popular with Chinese businessmen, overseas students and tourists. In Africa, Europe and America, "Northeast rice" even appeared in local supermarkets of these regions and provided the food for the local residents, indicating that the "Northeast rice" in the Northeastern Sanjiang Plain played an indispensable role in supplying food and exporting at home and abroad [4], serving food security worldwide [62].

5. Conclusions

Taking China's national commodity grain production base "the southern Sanjiang Plain of" as the study area, this study tracked the cropland structure change with 10-year intervals from 1990 to 2020, along with their impacts on the latest landscape spatial configuration information, crop structure and total grain production using the methods of land migration tracking, landscape ecological index and mathematical statistics. The main con-

clusions we obtained are displayed below from the perspective of land evolution, landscape and food security:

- (1) Coverage area of cropland continuously increased from 25,885.16 km² to 29,611.58 km², 30,391.87 km² and 31,144.46 km² in 1990, 2000, 2010 and 2020. Correspondingly, the land expansion rate constantly increased from 46.80 to 53.54%, 54.95 and 56.31%, showing that the proportion of cropland in the study area has exceeded half of the total area. Among the cropland structure, a sustained, rapid and intense paddy field expansion was monitored, with areas of 5513.41 km² in 2000 to 12,311.63 km² in 2020; in contrast, the area of upland crops decreased, with both values of 7.18 vs. 92.82% in 1990 to 39.53 vs. 60.47% in 2020.
- (2) Richness of landscape presented gradually complex characteristics, with SHDI from 0.258 to 0.671 during 1990–2020, leading to the fragmentation of PD with its value increasing from 0.158 in 1990 to 0.718 in 2020. This change weakened the connectivity among different land types and the dominance, and the degree of edge combination of patches continues to complicate. Landscape in this region has undergone complex changes with strong regularity.
- (3) Total grain production displayed a continuous increase, with the total production from 523.79×10^4 t to 1839.12×10^4 t, increasing by 3.51 times from 1990 to 2020. In addition, the crops experienced complex structural changes among the rice paddy, corn and soybean. For the impact of cropland on total grain production, the contribution rate of unchanged upland crops to grain increments reached 46.29%, considering that upland crops were the main cropland type in the whole study period, and the main conversion of internal cropland (i.e., the paddy fields converted from upland crops) contributed 12.17% from 1990 to 2020.

The conclusions and findings of this study from 1990 to 2020 provide the essential reference for the investigations on land evolution, landscape and food security regarding the cropland issues in China.

Author Contributions: Conceptualization, methodology, formal analysis, writing—original draft preparation, T.P.; writing—review and editing, T.P. and R.Z. All authors have read and agreed to the published version of the manuscript.

Funding: This project is funded by the Humanity and Social Science Youth Foundation of the Ministry of Education of China (Grant No. 21YJCZH111).

Institutional Review Board Statement: Not applicable.

Informed Consent Statement: Not applicable.

Data Availability Statement: Not applicable.

Conflicts of Interest: The authors declare no conflict of interest.

References

1. Su, Y.; Qian, K.; Lin, L.; Wang, K.; Guan, T.; Gan, M. Identifying the driving forces of non-grain production expansion in rural China and its implications for policies on cultivated land protection. *Land Use Policy* **2020**, *92*, 104435. [[CrossRef](#)]
2. Liu, G.; Zhang, L.; Zhang, Q.; Musyimi, Z. The response of grain production to changes in quantity and quality of cropland in Yangtze River Delta, China. *J. Sci. Food Agric.* **2015**, *95*, 480–489. [[CrossRef](#)] [[PubMed](#)]
3. Aubry, C.; Kebir, L. Shortening food supply chains: A means for maintaining agriculture close to urban areas? The case of the French metropolitan area of Paris. *Food Policy* **2013**, *41*, 85–93. [[CrossRef](#)]
4. Pan, T.; Zhang, C.; Kuang, W.; De Maeyer, P.; Kurban, A.; Hamdi, R.; Du, G. Time tracking of different cropping patterns using Landsat images under different agricultural systems during 1990–2050 in Cold China. *Remote Sens.* **2018**, *10*, 2011. [[CrossRef](#)]
5. Wei, Y.D.; Ye, X. Urbanization, urban land expansion and environmental change in China. *Stoch. Environ. Res. Risk Assess.* **2014**, *28*, 757–765. [[CrossRef](#)]
6. Ashraf, M.A.; Mohd Hanafiah, M. Sustaining life on earth system through clean air, pure water, and fertile soil. *Environ. Sci. Pollut. Res.* **2019**, *26*, 13679–13680. [[CrossRef](#)]
7. Vasco, C.; Torres, B.; Jácome, E.; Torres, A.; Eche, D.; Velasco, C. Use of chemical fertilizers and pesticides in frontier areas: A case study in the Northern Ecuadorian Amazon. *Land Use Policy* **2021**, *107*, 105490. [[CrossRef](#)]

8. Lamichhane, J.R.; Aubertot, J.-N.; Begg, G.; Birch, A.N.E.; Boonekamp, P.; Dachbrodt-Saaydeh, S.; Hansen, J.G.; Hovmøller, M.S.; Jensen, J.E.; Jørgensen, L.N. Networking of integrated pest management: A powerful approach to address common challenges in agriculture. *Crop Protect.* **2016**, *89*, 139–151. [[CrossRef](#)]
9. Li, S.; Li, X.; Sun, L.; Cao, G.; Fischer, G.; Tramberend, S. An estimation of the extent of cropland abandonment in mountainous regions of China. *Land Degrad. Dev.* **2018**, *29*, 1327–1342. [[CrossRef](#)]
10. Olsen, V.M.; Fensholt, R.; Olofsson, P.; Bonifacio, R.; Butsic, V.; Druce, D.; Ray, D.; Prishchepov, A.V. The impact of conflict-driven cropland abandonment on food insecurity in South Sudan revealed using satellite remote sensing. *Nat. Food* **2021**, *2*, 990–996. [[CrossRef](#)]
11. Xu, X.; Tang, Q. Spatiotemporal variations in damages to cropland from agrometeorological disasters in mainland China during 1978–2018. *Sci. Total Environ.* **2021**, *785*, 147247. [[CrossRef](#)] [[PubMed](#)]
12. Mechiche-Alami, A.; Abdi, A.M. Agricultural productivity in relation to climate and cropland management in West Africa. *Sci. Rep.* **2020**, *10*, 1–10.
13. Hernandez-Ramirez, G.; Hatfield, J.L.; Parkin, T.B.; Sauer, T.J.; Prueger, J.H. Carbon dioxide fluxes in corn–soybean rotation in the midwestern US: Inter-and intra-annual variations, and biophysical controls. *Agric. For. Meteorol.* **2011**, *151*, 1831–1842. [[CrossRef](#)]
14. Zhao, X.; Pu, C.; Ma, S.-T.; Liu, S.-L.; Xue, J.-F.; Wang, X.; Wang, Y.-Q.; Li, S.-S.; Lal, R.; Chen, F. Management-induced greenhouse gases emission mitigation in global rice production. *Sci. Total Environ.* **2019**, *649*, 1299–1306. [[CrossRef](#)] [[PubMed](#)]
15. Kumar, S.S.; Kumar, A.; Singh, S.; Malyan, S.K.; Baram, S.; Sharma, J.; Singh, R.; Pugazhendhi, A. Industrial wastes: Fly ash, steel slag and phosphogypsum-potential candidates to mitigate greenhouse gas emissions from paddy fields. *Chemosphere* **2020**, *241*, 124824. [[CrossRef](#)]
16. Watson, R.T.; Noble, I.R.; Bolin, B.; Ravindranath, N.; Verardo, D.J.; Dokken, D.J. *Land Use, land-Use Change and Forestry: A Special Report of the Intergovernmental Panel on Climate Change*; Cambridge University Press: Cambridge, UK, 2000.
17. Rufino, I.A.A.; de Oliveira Galvão, C.; de Brito Leite Cunha, J.E. Land-Use Land Cover Change and Forestry (LULCCF). *Clim. Action* **2020**, *9*, 619–629.
18. Yao, Z.; Zhang, L.; Tang, S.; Li, X.; Hao, T. The basic characteristics and spatial patterns of global cultivated land change since the 1980s. *J. Geogr. Sci.* **2017**, *27*, 771–785. [[CrossRef](#)]
19. Hu, Q.; Wu, W.; Xiang, M.; Chen, D.; Long, Y.; Song, Q.; Liu, Y.; Lu, M.; Yu, Q. Spatio-temporal changes in global cultivated land over 2000–2010. *Sci. Agric. Sin.* **2018**, *51*, 1091–1105.
20. Minghong, T.; Yuanyuan, L. Spatial and temporal variation of cropland at the global level from 1992 to 2015. *J. Resour. Ecol.* **2019**, *10*, 235–245. [[CrossRef](#)]
21. Chen, Y.; Xie, W.; Xu, X. Changes of population, built-up land, and cropland exposure to natural hazards in China from 1995 to 2015. *Int. J. Disaster Risk Sci.* **2019**, *10*, 557–572. [[CrossRef](#)]
22. Lichtenberg, E.; Ding, C. Assessing farmland protection policy in China. *Land Use Policy* **2008**, *25*, 59–68. [[CrossRef](#)]
23. Pan, T.; Zhang, C.; Kuang, W.; Luo, G.; Du, G.; DeMaeyer, P.; Yin, Z. A large-scale shift of cropland structure profoundly affects grain production in the cold region of China. *J. Clean. Prod.* **2021**, *307*, 127300. [[CrossRef](#)]
24. Jin, X.; Shao, Y.; Zhang, Z.; Resler, L.M.; Campbell, J.B.; Chen, G.; Zhou, Y. The evaluation of land consolidation policy in improving agricultural productivity in China. *Sci. Rep.* **2017**, *7*, 1–9.
25. Yao, S.; Colman, D.R. Chinese agricultural policies and agricultural reforms. *Oxf. Agrar. Stud.* **1990**, *18*, 23–34. [[CrossRef](#)]
26. Martin, W. Implications of reform and WTO accession for China’s agricultural policies. *Econ. Trans.* **2001**, *9*, 717–742. [[CrossRef](#)]
27. Peng, Z.; Wenhui, L.; Jun, S.; Pearson, S.; Hongsheng, Y. Natural coast protection and use in China: Implications of resource protection “Redline” policies. *Coast. Manag.* **2016**, *44*, 21–35. [[CrossRef](#)]
28. Chen, M.; Liu, W.; Lu, D. Challenges and the way forward in China’s new-type urbanization. *Land Use Policy* **2016**, *55*, 334–339. [[CrossRef](#)]
29. Cheng, Y.; Zhang, P.; Zhang, H. Variation character of grain yield per unit area in main grain-producing area of Northeast China. *Chin. Geogr. Sci.* **2007**, *17*, 110–116. [[CrossRef](#)]
30. Liu, Y.; Wang, D.; Gao, J.; Deng, W. Land use/cover changes, the environment and water resources in Northeast China. *Environ. Manag.* **2005**, *36*, 691–701. [[CrossRef](#)]
31. Wang, Y.; Zhou, L.; Ping, X.; Jia, Q.; Li, R. Ten-year variability and environmental controls of ecosystem water use efficiency in a rainfed maize cropland in Northeast China. *Field Crops Res.* **2018**, *226*, 48–55. [[CrossRef](#)]
32. Chen, F.; Fu, B.; Xia, J.; Wu, D.; Wu, S.; Zhang, Y.; Sun, H.; Liu, Y.; Fang, X.; Qin, B. Major advances in studies of the physical geography and living environment of China during the past 70 years and future prospects. *Sci. China Earth Sci.* **2019**, *62*, 1665–1701. [[CrossRef](#)]
33. Ye, Y.; Fang, X.; Ren, Y.; Zhang, X.; Chen, L. Cropland cover change in Northeast China during the past 300 years. *Sci. China Ser. D Earth Sci.* **2009**, *52*, 1172–1182. [[CrossRef](#)]
34. Liu, J.; Kuang, W.; Zhang, Z.; Xu, X.; Qin, Y.; Ning, J.; Zhou, W.; Zhang, S.; Li, R.; Yan, C. Spatiotemporal characteristics, patterns, and causes of land-use changes in China since the late 1980s. *J. Geogr. Sci.* **2014**, *24*, 195–210. [[CrossRef](#)]
35. Zhu, Z. Science of Landsat analysis ready data. *Remote Sens.* **2019**, *11*, 2166. [[CrossRef](#)]
36. Deng, X.; Huang, J.; Rozelle, S.; Uchida, E. Cultivated land conversion and potential agricultural productivity in China. *Land Use Policy* **2006**, *23*, 372–384. [[CrossRef](#)]

37. Fragstats v4: Spatial Pattern Analysis Program for Categorical and Continuous Maps. Available online: <http://www.umass.edu/landeco/research/fragstats/fragstats.html> (accessed on 18 February 2022).
38. Liu, J.; Kang, J.; Behm, H.; Luo, T. Effects of landscape on soundscape perception: Soundwalks in city parks. *Landsc. Urban Plan.* **2014**, *123*, 30–40. [[CrossRef](#)]
39. Kindlmann, P.; Burel, F. Connectivity measures: A review. *Landsc. Ecol.* **2008**, *23*, 879–890. [[CrossRef](#)]
40. McGarigal, K.; Marks, B.J. *Spatial Pattern Analysis Program for Quantifying Landscape Structure*; Gen. Technol. Rep. PNW-GTR-351; US Department of Agriculture, Forest Service, Pacific Northwest Research Station: Portland, OR, USA, 1995; pp. 1–122.
41. Edwards, A.W.; Cavalli-Sforza, L.L. A method for cluster analysis. *Biometrics* **1965**, *21*, 362–375. [[CrossRef](#)]
42. Liu, J.; Liu, M.; Tian, H.; Zhuang, D.; Zhang, Z.; Zhang, W.; Tang, X.; Deng, X. Spatial and temporal patterns of China's cropland during 1990–2000: An analysis based on Landsat TM data. *Remote Sens. Environ.* **2005**, *98*, 442–456. [[CrossRef](#)]
43. Huang, J.; Tu, Z.; Lin, J. Land-use dynamics and landscape pattern change in a coastal gulf region, southeast China. *Int. J. Sustain. Dev. World Ecol.* **2009**, *16*, 61–66. [[CrossRef](#)]
44. Bai, Y.; Dai, J.; Huang, W.; Tan, T.; Zhang, Y. Water conservation policy and agricultural economic growth: Evidence of grain to green project in China. *Urban Clim.* **2021**, *40*, 100994. [[CrossRef](#)]
45. Liu, J.; Zhang, Z.; Xu, X.; Kuang, W.; Zhou, W.; Zhang, S.; Li, R.; Yan, C.; Yu, D.; Wu, S. Spatial patterns and driving forces of land use change in China during the early 21st century. *J. Geogr. Sci.* **2010**, *20*, 483–494. [[CrossRef](#)]
46. Chong, L.; Liu, H.-J.; Qiang, F.; Guan, H.-X.; Qiang, Y.; Zhang, X.-L.; Kong, F.-C. Mapping the fallowed area of paddy fields on Sanjiang Plain of Northeast China to assist water security assessments. *J. Integr. Agric.* **2020**, *19*, 1885–1896.
47. Wang, X.; Pan, T.; Pan, R.; Chi, W.; Ma, C.; Ning, L.; Wang, X.; Zhang, J. Impact of Land Transition on Landscape and Ecosystem Service Value in Northeast Region of China from 2000–2020. *Land* **2022**, *11*, 696. [[CrossRef](#)]
48. Chen, C.; Park, T.; Wang, X.; Piao, S.; Xu, B.; Chaturvedi, R.K.; Fuchs, R.; Brovkin, V.; Ciais, P.; Fensholt, R. China and India lead in greening of the world through land-use management. *Nat. Sustain.* **2019**, *2*, 122–129. [[CrossRef](#)]
49. He, G.; Zhao, Y.; Wang, L.; Jiang, S.; Zhu, Y. China's food security challenge: Effects of food habit changes on requirements for arable land and water. *J. Clean. Prod.* **2019**, *229*, 739–750. [[CrossRef](#)]
50. Yang, C.; Jiang, X.; Du, H.; Li, Q.; Zhang, Z.; Qiu, M.; Yu, C. A review: Achievements and new obstacles in China's food security revealed by grain and animal meat production. In Proceedings of the IOP Conference Series: Earth and Environmental Science, Surakarta, Indonesia, 24–25 August 2021; p. 012025.
51. Wang, J.; Zhang, Z.; Liu, Y. Spatial shifts in grain production increases in China and implications for food security. *Land Use Policy* **2018**, *74*, 204–213. [[CrossRef](#)]
52. Ge, D.; Long, H.; Zhang, Y.; Ma, L.; Li, T. Farmland transition and its influences on grain production in China. *Land Use Policy* **2018**, *70*, 94–105. [[CrossRef](#)]
53. Gong, B. Agricultural reforms and production in China: Changes in provincial production function and productivity in 1978–2015. *J. Dev. Econ.* **2018**, *132*, 18–31. [[CrossRef](#)]
54. Li, S.; Zhang, D.; Xie, Y.; Yang, C. Analysis on the spatio-temporal evolution and influencing factors of China's grain production. *Environ. Sci. Pollut. Res.* **2022**, *29*, 23834–23846. [[CrossRef](#)]
55. Hejazi, M.; Marchant, M.A. China's evolving agricultural support policies. *Choices* **2017**, *32*, 1–7.
56. Liu, Y.; Fang, F.; Li, Y. Key issues of land use in China and implications for policy making. *Land Use Policy* **2014**, *40*, 6–12. [[CrossRef](#)]
57. Zhang, Z.; Lu, C. Clustering analysis of soybean production to understand its spatiotemporal dynamics in the North China Plain. *Sustainability* **2020**, *12*, 6178. [[CrossRef](#)]
58. Yang, X.; Liu, Y.; Bai, W.; Liu, B. Spatiotemporal assessment of drought related to soybean production and sensitivity analysis in Northeast China. *J. Appl. Meteorol. Climatol.* **2017**, *56*, 937–952. [[CrossRef](#)]
59. Liu, Z.; Yang, P.; Wu, W.; You, L. Spatiotemporal changes of cropping structure in China during 1980–2011. *J. Geogr. Sci.* **2018**, *28*, 1659–1671. [[CrossRef](#)]
60. Zhang, G.; Xiao, X.; Biradar, C.M.; Dong, J.; Qin, Y.; Menarguez, M.A.; Zhou, Y.; Zhang, Y.; Jin, C.; Wang, J. Spatiotemporal patterns of paddy rice croplands in China and India from 2000 to 2015. *Sci. Total Environ.* **2017**, *579*, 82–92. [[CrossRef](#)]
61. Fraser, E.D. The challenge of feeding a diverse and growing population. *Physiol. Behav.* **2020**, *221*, 112908. [[CrossRef](#)]
62. Van den Broeck, G.; Maertens, M. Horticultural exports and food security in developing countries. *Glob. Food Secur.* **2016**, *10*, 11–20. [[CrossRef](#)]